



**UNIVERSIDAD DE INVESTIGACIÓN DE
TECNOLOGÍA EXPERIMENTAL YACHAY**

Escuela de Ciencias Biológicas e Ingeniería

**TÍTULO: Systematics, Phylogeny, and X-ray Microtomography
of a New Amphibian Species of the Genus *Pristimantis* from
Cordillera del Cóndor, Ecuador (Anura: Strabomantidae)**

Trabajo de Integración Curricular presentado como requisito para la
obtención del título en Ciencias Biológicas

Autora:

Torres Constante Karen Odalys

Tutor:

Ph.D. Tellkamp Tietz Markus Patricio

Co-Tutor:

Ph.D. Ron Melo Santiago Rafael

Urququí, Julio 2020

SECRETARÍA GENERAL
(Vicerrectorado Académico/Cancillería)
ESCUELA DE CIENCIAS BIOLÓGICAS E INGENIERÍA
CARRERA DE BIOLOGÍA
ACTA DE DEFENSA No. UITEY-BIO-2020-00021-AD

A los 29 días del mes de mayo de 2020, a las 15:00 horas, de manera virtual mediante videoconferencia, y ante el Tribunal Calificador, integrado por los docentes:

Presidente Tribunal de Defensa Dr. CASTILLO MORALES, JOSE ANTONIO , Ph.D.

Miembro No Tutor Dra. SPENCER VALERO, LILIAN MARITZA , Ph.D.

Tutor Dr. TELLKAMP TIETZ, MARKUS PATRICIO , Ph.D.

El(la) señor(ita) estudiante **TORRES CONSTANTE, KAREN ODALYS**, con cédula de identidad No. **1717291312**, de la **ESCUELA DE CIENCIAS BIOLÓGICAS E INGENIERÍA**, de la Carrera de **BIOLOGÍA**, aprobada por el Consejo de Educación Superior (CES), mediante Resolución **RPC-SO-37-No.438-2014**, realiza a través de videoconferencia, la sustentación de su trabajo de titulación denominado: **Systematics, Phylogeny, and X-ray Microtomography of a New Amphibian Species of the Genus Pristimantis from Cordillera del Cóndor, Ecuador (Anura: Strabomantidae)**, previa a la obtención del título de **BIÓLOGO/A**.

El citado trabajo de titulación, fue debidamente aprobado por el(los) docente(s):

Tutor Dr. TELLKAMP TIETZ, MARKUS PATRICIO , Ph.D.

Y recibió las observaciones de los otros miembros del Tribunal Calificador, las mismas que han sido incorporadas por el(la) estudiante.

Previamente cumplidos los requisitos legales y reglamentarios, el trabajo de titulación fue sustentado por el(la) estudiante y examinado por los miembros del Tribunal Calificador. Escuchada la sustentación del trabajo de titulación a través de videoconferencia, que integró la exposición de el(la) estudiante sobre el contenido de la misma y las preguntas formuladas por los miembros del Tribunal, se califica la sustentación del trabajo de titulación con las siguientes calificaciones:

Tipo	Docente	Calificación
Miembro Tribunal De Defensa	Dra. SPENCER VALERO, LILIAN MARITZA , Ph.D.	10.0
Presidente Tribunal De Defensa	Dr. CASTILLO MORALES, JOSE ANTONIO , Ph.D.	9.0
Tutor	Dr. TELLKAMP TIETZ, MARKUS PATRICIO , Ph.D.	10.0

Lo que da un promedio de: **9.7 (Nueve punto Siete)**, sobre 10 (diez), equivalente a: **APROBADO**

Para constancia de lo actuado, firman los miembros del Tribunal Calificador, el/la estudiante y el/la secretario ad-hoc.



TORRES CONSTANTE, KAREN ODALYS
Estudiante

Dr. CASTILLO MORALES, JOSE ANTONIO , Ph.D.
Presidente Tribunal de Defensa

Firmado Digitalmente por: MARKUS PATRICIO
TELLKAMP TIETZ

Hora oficial Ecuador: 17/06/2020 18:08

Dr. TELLKAMP TIETZ, MARKUS PATRICIO, Ph.D.
Tutor

Dra. SPENCER VALERO, LILIAN MARITZA , Ph.D.
Miembro No Tutor

ALARCON FELIX, KARLA ESTEFANIA
Secretario Ad-hoc

AUTORÍA

Yo, **KAREN ODALYS TORRES CONSTANTE**, con cédula de identidad 1717291312, declaro que las ideas, juicios, valoraciones, interpretaciones, consultas bibliográficas, definiciones y conceptualizaciones expuestas en el presente trabajo; así cómo, los procedimientos y herramientas utilizadas en la investigación, son de absoluta responsabilidad de el/la autora (a) del trabajo de integración curricular. Así mismo, me acojo a los reglamentos internos de la Universidad de Investigación de Tecnología Experimental Yachay.

Quito, 11 de Julio del 2020.



Karen Odalys Torres Constante
CI:1717291312

AUTORIZACIÓN DE PUBLICACIÓN

Yo, **KAREN ODALYS TORRES CONSTANTE**, con cédula de identidad 1717291312, cedo a la Universidad de Tecnología Experimental Yachay, los derechos de publicación de la presente obra, sin que deba haber un reconocimiento económico por este concepto. Declaro además que el texto del presente trabajo de titulación no podrá ser cedido a ninguna empresa editorial para su publicación u otros fines, sin contar previamente con la autorización escrita de la Universidad.

Asimismo, autorizo a la Universidad que realice la digitalización y publicación de este trabajo de integración curricular en el repositorio virtual, de conformidad a lo dispuesto en el Art. 144 de la Ley Orgánica de Educación Superior

Quito, 11 de Julio del 2020.



Karen Odalys Torres Constante
CI:1717291312

Dedicatoria

Para mis abuelitos, mis padres, Francisco y mis tías Mery y Ceci por apoyarme incondicionalmente.

Karen Odalys Torres Constante

Agradecimientos

A Santiago Ron, Markus Tellkamp, a todos los miembros del Museo de Zoología QCAZ y de la Escuela de Ciencias de la Tierra y Energía de Yachay Tech por colaborarme durante este proceso.

Karen Odalys Torres Constante

Resumen en inglés

A new species of terrarana frog of the genus *Pristimantis* is described from the Reserva Ecológica El Quimi, Quimi Valley, in the southeastern Ecuadorian Andes. We also present an updated phylogeny for the subgenus *Huicundomantis*. The phylogeny shows that the new species belongs to the *P. cryptomelas* species group and is most closely related to *P. muscosus* and *P. barrigai*. *Pristimantis elquimi* **sp. n.** possesses similarity to *P. muscosus* and *P. spinosus* but differs from both species by having prominent cranial crests, vermiculations and a distinctive groin coloration. The new species was collected in a poorly sampled and unexplored area due to its difficult terrain. As a consequence, no information about its ecology and abundance was obtained. Accordingly, it is recommended to assign *P. elquimi* sp. n. to the Data Deficient Red List Category.

Keywords

Cordillera del Cóndor, osteology, phylogeny, *Pristimantis elquimi* **sp. n.**, systematics, taxonomy, X-ray microtomography.

Resumen en español

Una nueva especie de rana terrarana del género *Pristimantis* se describe, proveniente del sureste de los Andes ecuatorianos, en el Valle de Quimi, Reserva Ecológica El Quimi. También presentamos una filogenia actualizada para el subgénero *Huicundomantis*. La filogenia muestra que la nueva especie pertenece al grupo de especies de *P. cryptomelas* y está más estrechamente relacionada con *P. muscosus* y *P. barrigai*. *Pristimantis elquimi* **sp. n.** posee similitud con *P. muscosus* y *P. spinosus*, pero difiere de ambas especies por tener prominentes crestas craneales, vermiculaciones y una coloración diferente de la ingle. La nueva especie fue colectada en un área inaccesible, deficientemente muestreada e inexplorada. Como consecuencia, no hay información sobre su ecología y abundancia. Se recomienda asignar *P. elquimi* sp. n. a la Categoría Deficiente de Datos de la Lista Roja.

Palabras clave

Cordillera del Cóndor, osteología, filogenia, *Pristimantis elquimi* **sp. n.**, sistemática, taxonomía, microtomografía de Rayos X.

PUBLICATION MANUSCRIPT

Title

Systematics, phylogeny, and X-ray microtomography of a new amphibian species of the genus *Pristimantis* from Cordillera del Cóndor, Ecuador (Anura: Strabomantidae)

Journal:

ZooKeys

Authors

Odalys Torres and Santiago Ron

ORCID

<https://orcid.org/0000-0002-7263-6425>

<https://orcid.org/0000-0001-6300-9350>

E-mail

odalystorres20@gmail.com

santiago.r.ron@gmail.com

Address

Escuela de Ciencias Biológicas e Ingeniería, Universidad Yachay Tech, Hacienda San José,
Proyecto Yachay Urcuquí, Ecuador

Museo de Zoología, Escuela de Biología, Pontificia Universidad Católica del Ecuador,
Avenida 12 de Octubre y Roca, Apartado 17-01-2184, Quito, Ecuador

The present work has been written in ZooKeys journal format since the next page.

Systematics, phylogeny, and X-ray microtomography of a new amphibian species of the genus *Pristimantis* from Cordillera del Cóndor, Ecuador (Anura: Strabomantidae)

Odalys Torres¹, Santiago R. Ron²

1 School of Biological Sciences and Engineering, Universidad Yachay Tech, Hacienda San José, Proyecto Yachay, Urcuquí, Ecuador

2 Museo de Zoología, Escuela de Biología, Pontificia Universidad Católica del Ecuador, Avenida 12 de Octubre y Roca, Apartado 17-01-2184, Quito, Ecuador

Abstract

A new species of terrarana frog of the genus *Pristimantis* is described from the Reserva Ecológica El Quimi, Quimi Valley, in the southeastern Ecuadorian Andes. We also present an updated phylogeny for the subgenus *Huicundomantis*. The phylogeny shows that the new species belongs to the *P. cryptomelas* species group and is most closely related to *P. muscosus* and *P. barrigai*. *Pristimantis elquimi* **sp. n.** possesses similarity to *P. muscosus* and *P. spinosus* but differs from both species by having prominent cranial crests, vermiculations and a distinctive groin coloration. The new species was collected in a poorly sampled and unexplored area due to its difficult terrain. As a consequence, no information about its ecology and abundance was obtained. Accordingly, it is recommended to assign *P. elquimi* **sp. n.** to the Data Deficient Red List Category.

Resumen

Una nueva especie de rana terrarana del género *Pristimantis* se describe, proveniente del sureste de los Andes ecuatorianos, en el Valle de Quimi, Reserva Ecológica El Quimi. También presentamos una filogenia actualizada para el subgénero *Huicundomantis*. La filogenia muestra que la nueva especie pertenece al grupo de especies de *P. cryptomelas* y está más estrechamente relacionada con *P. muscosus* y *P. barrigai*. *Pristimantis elquimi* **sp. n.** posee similitud con *P. muscosus* y *P. spinosus* pero difiere de ambas especies por tener prominentes crestas craneales, vermiculaciones y una coloración diferente de la ingle. La nueva especie fue colectada en un área inaccesible, deficientemente muestreada e

inexplorada. Como consecuencia, no hay información sobre su ecología y abundancia. Se recomienda asignar *P. elquimi* sp. n. a la Categoría Deficiente de Datos de la Lista Roja.

Keywords

Cordillera del Cóndor, osteology, phylogeny, *Pristimantis elquimi* sp. n., systematics, taxonomy, X-ray microtomography.

Table of Contents

Dedicatoria.....	I
Agradecimientos.....	II
Resumen en inglés.....	III
Resumen en español.....	IV
Publication Manuscript.....	V
Abstract.....	1
Resumen.....	1
Objectives.....	3
General objective.....	3
Specific objectives.....	3
Introduction.....	3
Materials and Methods.....	6
Species sampling.....	6
Phylogenetic analyses.....	6
Morphological analyses.....	7
Osteological description.....	15
Results.....	15
Phylogenetic relationships.....	15
Morphometrics.....	17
Diagnosis.....	18
Comparison with other species.....	19
Description of the holotype.....	23
Variation.....	26

Osteological description.....	28
Skull.....	28
Postcranium.....	31
Manus and Pes.....	32
Distribution, natural story and conservation status.....	34
Etymology.....	35
Discussion.....	36
Conclusion.....	37
Acknowledgements.....	37
References.....	38
Supplementary Information.....	43

Objectives

General objective

Perform phylogenetic, morphological and osteological taxonomy approaches to delimit and determine the evolutionary relationships of a new species of *Pristimantis* genus of the Quimi Valley, Cordillera del Condor, Ecuador to consequently encourage the conservation of the species and its type locality.

Specific objectives

- Infer a molecular phylogeny that includes the new species of the genus *Pristimantis*.
- Perform a morphological and osteological characterization of the new species of *Pristimantis* from the southeast of Ecuador.
- Identify and define the diagnostic characteristics that distinguish the new species from the other *Pristimantis* species.

Introduction

The genus *Pristimantis* comprises 548 species of formally described anurans, making it the most diverse genus of amphibians (Lynch & Duellman 1997; Hedges, et al.2008; Frost 2016). The astounding diversity could be attributed to the appearance of new geographic barriers during the rise of the Andes during the Tertiary. Peak diversification of *Pristimantis* occurred during early-mid Paleogene (Duellman & Lehr 2009; Pinto-Sanchez

2012; Pyron 2014). *Pristimantis* are known for having direct development of terrestrial eggs and for its great ability to occupy new ecological niches, something not possible for species that rely on an aquatic environment for oviposition (Navarrete 2016). The number of described species in this group increases rapidly as shown by the 121 new species added within the last 10 years. Species discoveries in previously unexplored areas are especially frequent (Ron et al. 2018; AmphibiaWeb 2019).

Páez & Ron (2019) recently described the subgenus *Huicundomantis* comprising 48 species distributed in the Andes from central Ecuador to northern Peru. The subgenus consists of the *P. phoxocephalus* species and *P. cryptomelas* species groups. The *P. cryptomelas* group is formed by *P. cryptomelas* Lynch (1979), *P. galiardoi* Bustamante & Mendelson (2008), *P. muscosus* Duellman & Pramuk (1999), and *P. spinosus* Lynch (1979).

Duellman & Pramuk described *P. muscosus* in 1999 as part of the *Eleutherodactylus unistrigatus* species group based in four poorly preserved specimens. Its type locality are the eastern slopes of Abra Pardo Miguel, San Martín, Peru. It exhibits morphological similarities with *P. spinosus* (Lynch 1979: Fig.19; Duellman & Lehr 2009) and *P. cryptomelas* Duellman, & Lehr (2009). Later, it was assigned to the *P. unistrigatus* species group Hedges et al. (2008), but Padial et al. (2014) left it unassigned. The species was known from a single Peruvian location until Yanez-Muñoz et al. (2012) reported it from southern Ecuador based on morphological examination of five specimens from the Tapichalaca Reserve. More recently, one specimen of *P. muscosus* from Parque Nacional Yacuri in Ecuador was included in phylogenetic analyses Páez & Ron (2019), which suggested a close relationship with *P. spinosus* and *P. cryptomelas*.

The Quimi Valley is located in the Cordillera del Cóndor, a sub-Andean mountain chain located in southeastern Ecuador and northeastern Peru. The vegetation found there includes montane forests that are commonly stunted, and festooned with lichens and mosses. During two expeditions to the Reserva Biológica El Quimi, part of the Arca de Noé initiative (<https://bioweb.bio/colaboradores.html>), field herpetologists of Museo de Zoología of Pontificia Universidad Católica del Ecuador (PUCE) discovered a new species of *Pristimantis*, similar in morphology to *P. muscosus* (Figs. 1 and 2). In this study we present

a new phylogeny for the subgenus *Huicundomantis* as well as the description of the new species, including a description of its osteology examined by X-ray microtomography.

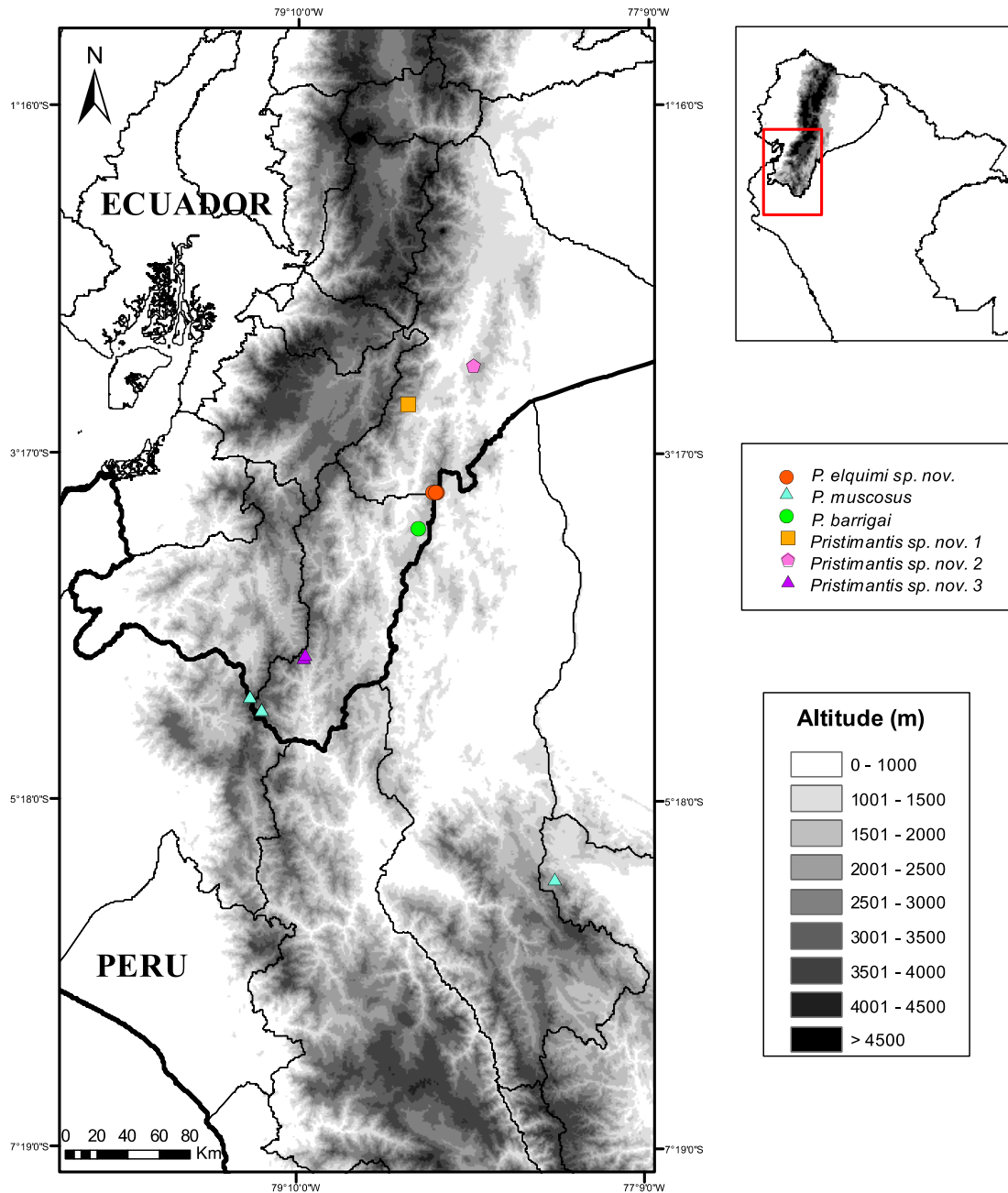


Figure 1. Map showing the type locality of *Pristimantis elquimi* sp. n. (QCAZ 68544, QCAZ 68545, QCAZ 68546) and collection sites of the most closely related species *P. muscosus* (KU 219482, MEPN 12346, QCAZ 61249, QCAZ 61250, QCAZ 61251, and

QCAZ 61252), *Pristimantis barrigai* (QCAZ 76129), *Pristimantis sp. nov. 1* (QCAZ 74686), *Pristimantis sp. nov. 2* (QCAZ 69189), and *Pristimantis sp. nov. 3* (QCAZ 54857).

Materials and methods

Species sampling

For the molecular phylogenetic analyses, we used 111 sequences of 87 individuals of putatively closely related species such as, *P. muscosus*, *P. spinosus*, *P. cryptomelas*, *P. barrigai*, *Pristimantis sp. nov. 1*, *Pristimantis sp. nov. 2*, and *Pristimantis sp. nov. 3*, and added sequences of 24 species as outgroup (20 *Pristimantis* spp., *Craugastor longirostris*, *Barycholos pulcher*, *Strabomantis sulcatus*, *Niceferonia sp.*). Our final dataset consists of sequences of 111 individuals from 81 localities. Sequences of 87 of these individuals were obtained from tissues deposited at the Museo de Zoología (QCAZ), Pontificia Universidad Católica del Ecuador (PUCE), representing 58 described and at least 6 undescribed species of *Pristimantis*. The remaining sequences from 12 species were obtained from GenBank (<http://www.ncbi.nlm.nih.gov/genbank>). Vouchers and GenBank accession numbers for all specimens are shown in Table 1.

Phylogenetic analyses

DNA was extracted using the guanidine thiocyanate protocol (M. Fujita, unpublished) with some modifications from liver or muscle tissue preserved in 95% ethanol or tissue storage buffer. Primers used for the PCR amplification of the below-listed loci are listed in Supplementary information 1. Amplicons were sequenced by the MacroGen Sequencing Team (MacroGen Inc. Seoul, Korea).

The phylogenetic analyses were based on a 3178 bp dataset containing DNA sequences of the mitochondrial genes 16S (1369 bp, partial sequence), tRNA^{Leu} (72 bp), NADH dehydrogenase subunit 1 ND1 (959 bp), tRNA^{Ile} (80 bp), tRNA^{Gln} (69 bp), and the nuclear gene RAG1 (625 bp). Alignment of the sequences was performed in GeneiousPro 5.4.6 (GeneMatters Corp.) with the plug-in MAFFT (Katoh et al. 2002), followed by manual alignment with Mesquite v.3.02 (Maddison and Maddison 2014). The aligned matrix is available at <http://zenodo.org>. The best partitioning scheme and fitting models for

molecular evolution for each branch were estimated with the IQ-TREE software (Nguyen et al. 2015). The spp command creates a file with the best partition and the MFP+MERGE command finds the best-fit model of molecular evolution for each partition.

For the ML analysis, we also used IQ-TREE (Nguyen et al. 2015), limiting the search to 3000 generations with non-parametric Shimodaira-Hasegawa Approximate Light Ratio Test (SH-ALrt; Guindon et al. 2010) for topology improvement. UFBoot2: Ultrafast Bootstrap (Minh et al. 2013; Hoang et al. 2018) values were obtained with 3000 pseudoreplicates maintaining the settings as for the random search. The 50% majority rule consensus for the bootstrap trees was obtained with IQ-TREE (Nguyen et al. 2015). Throughout the text, we considered that a node has reached high levels of support, given our data and chosen models, when a UFBoot value greater than 95% was obtained in for maximum likelihood values (difference less than 1%) with a SH-aLRT greater than 80%.

In order to identify candidate species, we calculated uncorrected p genetic distances for gene 16S (~1300 bp), within and between clades, with software Mesquite v. 3.6 (Maddison & Maddison 2018) for species discrimination see Supplementary Information 2.

Morphological analyses

We compared the morphology of the new species with closely related species based on our phylogeny (Fig. 3): *P. muscosus*, *P. spinosus*, *P. cryptomelas*, *P. barrigai*, *Pristimantis* sp. nov. 1, *Pristimantis* sp. nov. 2, and *Pristimantis* sp. nov. 3. The new species described here belongs to the subgenus *Huicundomantis* (Páez & Ron 2019). Therefore, we included all available GenBank sequences for that clade in addition to sequences of the new species, *P. barrigai*, and specimens of other morphologically similar species deposited in the QCAZ collection.

Photographs of preserved specimens were taken while these were submersed in ethanol to avoid reflections. We compared qualitative and quantitative morphological characters among clades. We examined 36 individuals belonging to nine species collected in southern Ecuador at elevations ranging from 230 to 4200 m.a.s.l. (Fig. 1). We used only adult specimens for these analyses but, when available, juveniles were examined to describe

morphological variation. Examined specimens are deposited at the collections of Museo de Zoología, Pontificia Universidad Católica del Ecuador (QCAZ), Escuela Politécnica Nacional, Ecuador (MEPN), Museo Ecuatoriano de Ciencias Naturales, Ecuador (MECN), and Natural History Museum, University of Kansas (KU).

We assessed sex and reproductive condition by determining the presence or absence of vocal sacs, vocal slits, and nuptial pads, and by gonadal inspection, except in the case of adult males possessing conspicuous deflated vocal sacs. For males, the presence of vocal sac, vocal slits, or nuptial pads was used as indicator of adulthood; when these characters were absent, we examined the gonads and categorized an individual as adult if the testes were swollen and enlarged. Adult females are identified by the presence of curved oviducts, and large ovarian eggs are indicators of adulthood (Duellman & Lehr 2009).

Diagnosis and description of species follow Duellman & Lehr (2009). The term “distinct” refers to a clearly visible character, and “indistinct” refers to a barely visible or variably non-present character. When referring to the tympanum state, we use “prominent” to denote that it protrudes from the skin surface; when referring to tubercles, we use “prominent” to imply they are conspicuous and elevated. Following Lynch and Duellman (1997), we qualify Toe V as slightly longer than Toe III when the distal end of Toe V does not reach the proximal edge of the distal subarticular tubercle on Toe IV when they are adpressed. Toe V is considered longer than Toe III when its distal end reaches the proximal edge of the distal subarticular tubercle in Toe IV and does not extend to its distal edge. Toe V is markedly longer than Toe III if the distal end of Toe V reaches, or extends beyond, the distal edge of the distal subarticular tubercle on Toe IV. Abbreviations used for quantitative descriptive characters are: (1) snout-vent length (SVL); (2) head width (HW); (3) head length (HL); (4) eye diameter (ED); (5) interorbital distance (IOD); (6) upper eyelid width (EW); (7) eye-nostril distance (END); (8) internarial distance (IND); (9) tympanic diameter (TY); (10) tympanum-eye distance (TED); (11) tibia length (TL); (12) foot length (FL; Duellman and Lehr 2009). All measurements were made with a digital caliper with an accuracy of 0.01 mm.

Table 1. GenBank accession numbers and vouchers of DNA sequences used in phylogenetic analyses (NGY=No GenBank Yet (to be added), NA=no accession number).

Species	Voucher	16S	ND1	RAG1	GenSeq Nomenclature
<i>Craugastor longirostris</i>	QCAZ 19764	NGY	NGY	NGY	NGY
<i>Barycholos pulcher</i>	KU 217781	NGY	NGY	NGY	NGY
<i>Niceferonia sp.</i>	QCAZ 45959	NGY	NGY	NGY	NGY
<i>Strabomantis sulcatus</i>	QCAZ 51260	NGY	NGY	NGY	NGY
<i>P. ardyae</i>	QCAZ 52498	NGY	NGY	NGY	NGY
<i>P. atillo</i>	QCAZ 42492	MK881442	NA	MK881342	genseq-2
<i>P. atratus</i>	QCAZ 45645	MK881473	MK881473	MK881366	genseq-4
<i>P. barrigai</i>	QCAZ 76129	NGY	NGY	NGY	NGY
<i>P. bicantus</i>	QCAZ 31986	MK881420	NA	MK881325	genseq-4
<i>P. buckleyi</i>	QCAZ 43174	NGY	NGY	NGY	NGY
	QCAZ 39658	NGY	NGY	NGY	NGY
	QCAZ 43157	NGY	NGY	NGY	NGY
	QCAZ 39690	NGY	NGY	NGY	NGY
	QCAZ 42372	NGY	NGY	NGY	NGY
<i>P. celator</i>	QCAZ 42366	NGY	NGY	NGY	NGY
	KU 177684	NGY	NGY	NGY	NGY

Species	Voucher	16S	ND1	RAG1	GenSeq Nomenclature
<i>P. chloronotus</i>	KU 202325	NGY	NGY	NGY	NGY
<i>P. chomskyi</i>	QCAZ 45666	MK881476	MK881476	MK881369	genseq-2
<i>P. colonensis</i>	QCAZ 53318	NGY	NGY	NGY	NGY
	QCAZ 46568	NGY	NGY	NGY	NGY
<i>P. cryptomelas</i>	QCAZ 45660	MK881475	MK881476	MK881368	genseq-4
<i>P. curtipes</i>	QCAZ 40722	NGY	NGY	NGY	NGY
	QCAZ 47121	NGY	NGY	NGY	NGY
<i>P. devillei</i>	QCAZ 40152	NGY	NGY	NGY	NGY
<i>P. duellmani</i>	WEC 53050	NGY	NGY	NGY	NGY
<i>P. elquimi</i> sp. nov.	QCAZ 68544	NGY	NGY	NGY	NGY
	QCAZ 69546	NGY	NGY	NGY	NGY
<i>P. eriphus</i>	QCAZ 45757	NGY	NGY	NGY	NGY
<i>P. festae</i>	KU218234	NGY	NGY	NGY	NGY
<i>P. gagliardoii</i>	QCAZ 46738	MK881480	NA	MK881372	genseq-2
<i>P. gentryi</i>	QCAZ 21021	NGY	NGY	NGY	NGY
	QCAZ 40736	NGY	NGY	NGY	NGY
	QCAZ 42714	NGY	NGY	NGY	NGY
	QCAZ 42581	NGY	NGY	NGY	NGY
<i>P. gloria</i>	QCAZ 16448	MK881402	MK881402	MK881316	genseq-2

Species	Voucher	16S	ND1	RAG1	GenSeq Nomenclature
	QCAZ 45129	NGY	NGY	NGY	NGY
<i>P. hampatusami</i>	QCAZ 58042	MK881504	MK881504	MK881387	genseq-3
	QCAZ 26642	NGY	NGY	NGY	NGY
<i>P. hernandezi</i>	JJM 210	NGY	NGY	NGY	NGY
<i>P. huicundo</i>	QCAZ 15392	NGY	NGY	NGY	NGY
<i>P. incanus</i>	QCAZ 59032	NGY	NGY	NGY	NGY
<i>P. inusitatus</i>	QCAZ 40149	NGY	NGY	NGY	NGY
<i>P. jimenezi</i>	QCAZ 45178	MK881468	MK881468	MK881362	genseq-2
<i>P. leoni</i>	KU 218227	NGY	NGY	NGY	NGY
<i>P. lividus</i>	QCAZ 46272	NGY	NGY	NGY	NGY
<i>P. llanganati</i>	QCAZ 46140	NGY	NGY	NGY	NGY
<i>P. lutzae</i>	QCAZ 32791	NGY	NGY	NGY	NGY
<i>P. multicolor</i>	QCAZ 47213	MK881488	NA	NA	genseq-1
<i>P. muscosus</i>	QCAZ 61249	NGY	NGY	NGY	NGY
	QCAZ 61252	NGY	NGY	NGY	NGY
<i>P. nangaritza</i>	QCAZ 41710	MK881436	MK881436	MK881336	genseq-1
<i>P. ocreatus</i>	QCAZ 13664	NGY	NGY	NGY	NGY
<i>P. ortizi</i>	QCAZ 49670	NGY	NGY	NGY	NGY
	QCAZ 70070	NGY	NGY	NGY	NGY

Species	Voucher	16S	ND1	RAG1	GenSeq Nomenclature
<i>P. phillipi</i>	QCAZ 37537	MK881426	MK881426	MK881331	genseq-3
<i>P. phoxocephalus</i>	QCAZ 58463	MK881507	MK881507	MK881389	genseq-3
<i>P. phyromerus</i>	QCAZ 13769	NGY	NGY	NGY	NGY
	QCAZ 38209	NGY	NGY	NGY	NGY
<i>P. pichincha</i>	QCAZ 11673	MK881399	MK88399	MK881313	genseq-4
<i>P. quincuagesimus</i>	QCAZ 24849	NGY	NGY	NGY	NGY
	QCAZ 35320	NGY	NGY	NGY	NGY
<i>P. riveti</i>	QCAZ 40012	NGY	NGY	NGY	NGY
<i>P. roni</i>	QCAZ 58924	NGY	NGY	NGY	NGY
	QCAZ 51996	NGY	NGY	NGY	NGY
	QCAZ 45941	NGY	NGY	NGY	NGY
<i>P. sobetes</i>	QCAZ 11737	MK881400	NA	MK881314	genseq-4
<i>P. spinosus</i>	KU218052	EF493673	NA	NA	genseq-4
<i>P. supernatis</i>	QCAZ 52278	NGY	NGY	NGY	NGY
	KU 202432	NGY	NGY	NGY	NGY
<i>P. surdus</i>	KU 177847	NGY	NGY	NGY	NGY
<i>P. teslai</i>	QCAZ 45029	NGY	NGY	NGY	NGY
	QCAZ 46213	MK881478	NA	NA	genseq-1
<i>P. thymalopsoides</i>	QCAZ 42972	NGY	NGY	NGY	NGY

Species	Voucher	16S	ND1	RAG1	GenSeq Nomenclature
<i>P. tinguinchaca</i>	QCAZ 31945	MK881418	MK881418	MK881323	genseq-3
<i>P. torresi</i>	QCAZ 47397	MK881492	MK881492	MK881380	genseq-2
<i>P. totoroii</i>	QCAZ 58425	MK881505	MK881505	MK881388	genseq-2
<i>P. truebae</i>	QCAZ 13752	NGY	NGY	NGY	NGY
	QCAZ 13782	NGY	NGY	NGY	NGY
	QCAZ 42997	NGY	NGY	NGY	NGY
	QCAZ 42547	NGY	NGY	NGY	NGY
	QCAZ 44994	NGY	NGY	NGY	NGY
	QCAZ 45197	NGY	NGY	NGY	NGY
<i>P. verdecundus</i>	QCAZ 12410	NGY	NGY	NGY	NGY
<i>P. verrucolatus</i>	QCAZ 32790	NGY	NGY	NGY	NGY
	QCAZ 46992	MK881484	MK881484	MK881376	genseq-2
<i>P. versicolor</i>	QCAZ 53999	NGY	NGY	NGY	NGY
	QCAZ 46310	MK881479	MK881479	MK881371	genseq-4
<i>P. vertebralis</i>	KU 177972	NGY	NGY	NGY	NGY
<i>P. yanezi</i>	QCAZ 46257	NGY	NGY	NGY	NGY
<i>P. yumbo</i>	QCAZ 42653	NGY	NGY	NGY	NGY
<i>Pristimantis</i> sp. nov. 1	QCAZ 74686	NGY	NGY	NGY	NGY
<i>Pristimantis</i> sp. nov. 2	QCAZ 69189	NGY	NGY	NGY	NGY

Species	Voucher	16S	ND1	RAG1	GenSeq Nomenclature	
<i>Pristimantis</i> sp. nov. 3	QCAZ 54847	NGY	NGY	NGY	NGY	
<i>Pristimantis</i> sp. CS1	QCAZ 54594	NGY	NGY	NGY	NGY	
	QCAZ 54595	NGY	NGY	NGY	NGY	
	QCAZ 54596	NGY	NGY	NGY	NGY	
<i>Pristimantis</i> sp. CS2	QCAZ 68550	NGY	NGY	NGY	NGY	
	QCAZ 68566	NGY	NGY	NGY	NGY	
	QCAZ 68558	NGY	NGY	NGY	NGY	
	QCAZ 68606	NGY	NGY	NGY	NGY	
	QCAZ 68565	NGY	NGY	NGY	NGY	
	QCAZ 68626	NGY	NGY	NGY	NGY	
	<i>Pristimantis</i> sp.	QCAZ 15909	NGY	NGY	NGY	NGY
		QCAZ 44989	NGY	NGY	NGY	NGY
QCAZ 43189		NGY	NGY	NGY	NGY	
KU 179221		NGY	NGY	NGY	NGY	
QCAZ 43504		NGY	NGY	NGY	NGY	
QCAZ 37700		NGY	NGY	NGY	NGY	
QCAZ 40321		NGY	NGY	NGY	NGY	
QCAZ 40311		NGY	NGY	NGY	NGY	

Osteological description

Osteological descriptions are based on X-ray microtomography images in TIFF format obtained using a SkyScan 1173 High Energy microCT, housed at the School of Earth Sciences, Energy and Environment, Yachay Tech University, Ecuador. The scan was performed by rotating the specimen by 180 degrees in steps of 0.2 degrees (source voltage of 70 kV and source current of 195 μ A) resulting in a pixel size of 35 μ m. Scan duration was 20 min and exposure time for each angle was 163 ms.

The frogs were placed in a low-density, completely sealed plastic bag. Parafilm was used to further seal the bag to prevent desiccation of the specimen. To maintain the sample in a vertical position and secure it to the base, we used G.U.M brand orthodontist rubber (Sunstar Suisse S.A.).

The 3D images were assembled using the software NRecon v. 1.7.4.2 (Bruker 2016) by implementing the Feldkamp algorithm (NRecon User Manual 2016). The images rendered by NRecon were saved in BMP format. We used the CTan (Bruker 2018) and CTvox software (Bruker 2016) for settings, visualization, and export of the 3D image to perform the osteological description. Osteological terminology follows Reyes et al. (2019).

Results

Phylogenetic relationships

In our phylogenomic analysis, we use a supermatrix which is made up of concatenated gene alignments. We generated partition schemes in which a substitution model can be specified for each gene or character set (as reports IQTREE). Partition models are estimated separately for each character set. For our concatenated matrix we use `-spp` that is the correct parameter for typical analysis with real data. The `-spp` parameter provides us with partition models that possess edge-link branch lengths and also allow each partition to have a different evolutionary speed (Chernomor et al. 2016). The best partition schemes and models for our concatenated matrix consisted of the following six: 16S (TIM2+F+I+G4), ND1 1st position (TVM+F+I+G4); ND1 2nd position (TPM3+F+I+G4); ND1 3rd position

(TIM3+F+I+G4); RAG1 3rd position (K2P+G4); RAG1 1st and 2nd position (TPM3u+F+R2) obtained with IQTREE (Nguyen et al. 2015).

Presently, the genus *Pristimantis* is divided into 2 subgenera: *Pristimantis* and *Hypodictyon*. The creation of the new subgenus *Huicundomantis* has contributed to establish the monophyly of all *Pristimantis* subgenera. Our phylogeny exhibits the same topology as the one reported by Páez and Ron (2019). *Pristimantis elquimi* sp. n. belongs to the *P. cryptomelas* species group (Fig. 3). We also present the position of three *Pristimantis* ssp. obtained in Tinajillas (*Pristimantis* sp. nov. 1, QCAZ 74686), Cutucú (*Pristimantis* sp. nov. 2, QCAZ 69189) and Tapichalaca (*Pristimantis* sp. nov. 3, QCAZ 54847). This clade is distributed in southeastern Ecuador and northern Peru, and includes *P. muscosus*, *Pristimantis* sp. nov. 3 and *P. barrigai*, the sister clade of *P. elquimi* sp. n (Fig.3). The phylogeny does not strongly support *Pristimantis* sp. nov. 3 and *P. barrigai* to be different species. We still consider *Pristimantis* sp. nov. 3 a new species on the basis of genetic distances (Supp. Info. 2) and morphological examination. The phylogeny for the *P. cryptomelas* group have considerable UF bootstrap support with the exception of *P. barrigai* and *Pristimantis* sp. nov. 3 branch which suggest that for better accuracy a bigger sampling of this species is needed. Moreover, the branch's support of *P. elquimi* sp. n. phylogenetic relationship is greater than 95%. Evidently, the low branch support for the *Pristimantis* sp. nov. 3 and *P. barrigai* clade requires further study. Genetic distances and morphological differences confirm that *P. elquimi* sp. n. is a new species, described later on in the present work (Table 1).



Figure 3. Phylogeny of the subgenus *Huicundomantis* showing the systematic position of *Pristimantis elquimi* sp. n. (orange). aLRT (%) values followed by UFBoot values are shown next to the corresponding branches. The phylogeny is based on 3178 bp of mitochondrial (gene fragments 16S and ND1) and nuclear (RAG1) DNA sequences. “KU218052/EF493673” is a specimen from the University of Kansas Natural History Museum collection, and “QCAZ” corresponds to specimens from the Museo de Zoología of the Pontificia Universidad Católica del Ecuador (PUCE). The collection number, identification, province and locality of the samples are shown next to each terminal; all samples are from Ecuador. Outgroup is not shown. Abbreviations: CS = candidate species.

Morphometrics

Systematic account

Pristimantis elquimi sp. nov.

Common name: English: El Quimi Rain Frog. Spanish: Cutín de El Quimi

Holotype: QCAZ 68544 (Field number. SC-PUCE 59150, Fig. 1), an adult female from Ecuador, Morona Santiago Province, Gualaquiza, Bomboiza, the upper part of the Reserva Ecológica El Quimi (-3.5187S; -78.3927O, 1984 m), collected by Diego Almeida, Darwin Núñez, Eloy Nusirquia, Alex Achig, and Ricardo Gavilanes on November 28th, 2017.

Paratopotypes (2 specimens). QCAZ 68545 adult male, QCAZ 68546 sub-adult male, both collected with the holotype.

Diagnosis. A species of *Pristimantis* characterized by the following combination of characters. (1) *P. elquimi* sp. n. possesses T-shaped terminal phalanges, and Toe V that is longer than Toe III. (2) Skin of dorsum is shagreen, highly tuberculate in the posterior half and slightly tuberculate in the anterior half. Two medial tubercles are vertically aligned at the top of the head, one interorbitally, and the other one anteriorly located that is vertically aligned with the interorbital tubercle and horizontally aligned with the anterior border of the eyes; skin of the venter is areolate to weakly areolate; discoidal fold is distinct; dorsolateral folds are absent. (3) Tympanic membrane and tympanic annulus, respectively, are prominent, upper margin of tympanic annulus is covered by a supratympanic fold. (4) Snout is short, rounded in lateral and dorsal view. (5) Upper eyelid bear three to four prominent, rounded tubercles, surrounded by several smaller, rounded tubercles; cranial crests are present. (6) Dentigerous process of vomer is oblique and posteriorly located to the level of choanae, narrowly separated, but almost in contact; vomerine teeth in males are indistinct and several small rounded teeth 4-6 in each vomer are present in females. (7) Vocal slits and nuptial pads absent. (8) Finger I shorter than Finger II; discs of digits expanded, semitruncated. (9) Fingers have narrow lateral fringes. (10) Three low and rounded ulnar and carpal tubercles are present. (11) Heel bears a prominent conical tubercle surrounded by small and rounded scattered tubercles; inner tarsal fold is absent. (12) Inner metatarsal tubercle is prominent, elliptical, and three times bigger than the outer metatarsal tubercle; outer metatarsal tubercle is small and ovoid; few rounded and small supernumerary plantar tubercles are present. (13) Toes possess lateral fringes; basal toe webbing is absent; Toe IV is longer than toe III (disc on toe III reaches the middle of the distal subarticular tubercle on Toe IV); Toe IV is longer than Toe V (disc on Toe III reaches the middle of the penultimate subarticular tubercle on Toe IV, disc on Toe V does

reach the subarticular tubercle on Toe IV); toe discs are slightly smaller than those on fingers (Fig. 4). (14) In life, the dorsum is pale to dark brown with irregular, darker-colored marbling; a dark brown interorbital mark is present; the scapula bears dermal crests that can be W-shaped in juveniles or possess a scatter W-shaped structure (> < shape with an internal small V-shaped scapular fold) in adults; the sides of the head are pale to dark brown with vertical labial bars; flanks are pale brown with darker brown blotches and flecks; groin is dark brown with white to cream spots and bars; hindlimbs show transverse darker brown bars, posterior surface of the thighs are black with white spots; venter is cream with dark to pale brown mottling up to the throat; iris is brownish coppery red. (15) SVL is 31.57 mm in adult female (n=1) and 26.4 mm (n=2) in adult male.

Comparison with other species. In this section, coloration refers to live individuals unless otherwise noticed. *Pristimantis elquimi* sp. n. is similar to congeneric species characterized by a spiny appearance (i.e. presence of conical upper eyelid, ulnar and heel tubercles). We differentiate *Pristimantis elquimi* sp. n. from each of those species below.

Pristimantis elquimi sp. n. can be differentiated from *P. spinosus*, *P. cryptomelas* and *P. barrigai* by its interorbital tubercle, broad dorsolateral vermiculations, and dermal crests (Fig. 3). *Pristimantis elquimi* sp. n. presents a prominent and rounded interorbital tubercle (absent in *P. muscosus* and *P. spinosus*). Dorsal texture of *P. elquimi* sp. n is composed of small rounded tubercles (prominent tubercles present in *P. spinosus*). Vermiculations on *P. elquimi*. sp. n. are broad, creamy and sometimes absent (*P. muscosus* often bears white narrow dorsolateral vermiculation), sometimes dark brown in *P. spinosus*, and creamy to dark brown in *P. elquimi*. Presence of a dark interorbital bar, the scapula bears dermal crests that can be W-shaped in juveniles or scatter W-shaped (> < shape with an internal small V-shaped scapular fold) in adults in *P. elquimi* sp. n. (blunt or absent in *P. muscosus* and blunt in *P. spinosus*). Cranial crests and dermal crests present in *P. elquimi* sp. nov. (cranial crests present in *P. spinosus* and dermal crests present in *P. cryptomelas*). Postocular folds in *P. elquimi* sp. n. are blunt (absent in *P. muscosus*). Snout shape rounded in *P. elquimi* sp. n. (subacuminate in *P. cryptomelas* and *P. spinosus* and bluntly rounded in *P. muscosus*; Fig. 3). The variation of dorsal and ventral skin coloration and texture, groin and hidden surfaces, and other important traits are shown in Table 2.

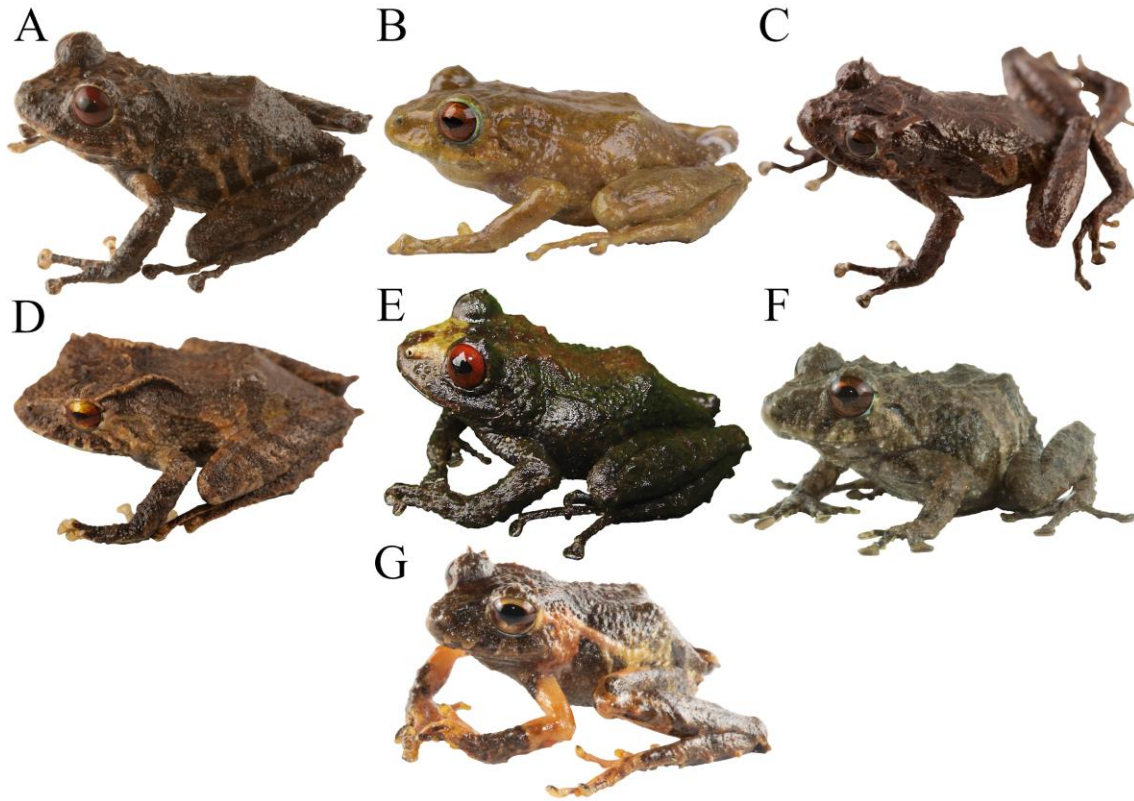


Figure 2. Coloration in life of *P. elquimi* sp. n. and similar congeners. **A** *Pristimantis elquimi* sp. n., QCAZ 68544, SVL=31.57 mm, adult female; **B** *Pristimantis muscosus*, QCAZ 61252, SVL=21.92 mm, adult male; **C** *Pristimantis spinosus*, QCAZ 42571, SVL=17.25, juvenile; **D** *Pristimantis cryptomelas*, QCAZ 45660, SVL=18.46, juvenile; **E** *Pristimantis barrigai*, QCAZ 76129, SVL=25.92 mm, adult female; **F** *Pristimantis* nov. 1, QCAZ 69189, SVL=30.06 mm, adult female; **G** *Pristimantis* nov. 2, QCAZ 74686, SVL=24.62, juvenile female.

Table 2. Qualitative morphological characters of the most related species to *P. elquimi* sp. n. based on Bioweb data (<https://bioweb.bio/portal/>) and specimen's examination.

<i>Morphological traits</i>	<i>P. elquimi</i> sp. n.	<i>P. muscosus</i>	<i>P. spinosus</i>	<i>P. cryptomelas</i>	<i>P. barrigai</i>
Dorsal texture	Shagreen with scattered small tubercles	Smooth with scattered small tubercles	Smooth with scattered small tubercles	Areolate with conical tubercles	Areolate with scattered small tubercles
Dorsal coloration	Pale to dark brown with irregular darker markings	Green with many black spots and irregular white lines	Pale to dark brown with darker chevrons	Pale brown to creamy orange	Olive brown
Post ocular fold/ridge	+	-	+	+	+
Ventral texture	Areolate	Areolate	Strongly areolate	Areolate	Areolate
Ventral coloration	Dark brown mottling on a cream background	Mostly tan with dark brown background	Cream with dark brown irregular markings	Black with white markings to black reticulations	Black
Groin and hidden surfaces	Light brown with darker brown blotches	Orange to yellow spots	Black with white spots	Black often with yellow markings	Olive brown

Snout dorsolateral shape	Rounded (dorsal and lateral)	Long, bluntly, rounded, (dorsal), rounded (lateral)	Sub-acuminated (dorsal), truncated (lateral)	Sub-acuminated (dorsal), rounded (lateral)	Slightly rounded (dorsal), rounded (lateral)
Tympanic membrane and annulus	Prominent (30% to 40% of the eye diameter)	Distinctive	Prominent (1/5 to 2/5 of length in males and 1/3 to 2/3 in females)	Prominent (30% to 40% of the eye diameter)	Distinctive with a small tympanic annulus
Vermiculations	Often broad, creamy to dark brown lateroventral	Often narrow white dorsolateral	-	Diffuse dorsolateral	-
Disc shape	Expanded and semi truncated	Expanded semi truncated	Expanded and truncated	Broad and elliptic	Expanded and semi truncated
Size comparison (Adult females)	31.6	29.6 – 46.1	28.3 – 34.5	38.6 – 39.5	31.5
Cranial crests	-	-	+	-	-
Dermal crests	+	-	-	+	-
Interorbital bar	+	+/-	-	-	-
Discoidal fold	Evident	Indistinctive	Indistinctive	Prominent	Evident
Ulnar tubercles	Prominent	Indistinctive	Prominent	Prominent	Evident
Iris	Coppery not metallic red	Yellowish metallic red	Brownish metallic red	Metallic yellow and red	Brilliant red

Description of the holotype. Adult female. Measurements (in mm): SVL 31.57; tibia length 18.09; foot length 14.53; head length 10.05; head weight 11.51; eye diameter 4.72; tympanum diameter 1.1; interorbital distance 3.4; upper eyelid width 3.13; internarial distance 2.04; eye-nostril distance 3.82; tympanum-eye distance 1.45. Head is wider than long and as wide as body, head width is 36% of SVL and head length 32% of SVL. Canthus rostralis is distinct; snout is short and rounded in lateral and dorsal views; loreal region is distinct and lips rounded; upper eyelid bears a prominent conical tubercle surrounded by lower, rounded tubercles, and upper eyelid width is 87% of IOD. Tympanic annulus is distinct, tympanum diameter is 30% of the eye diameter, tympanic membrane is present, tympanum-eye is 92% of tympanum diameter; postictal tubercles are present, few and small. Choanae are large, ovoid, slightly separated but not concealed by palatal shelf of maxilla; dentigerous process of vomer is oblique, located at the posteromedial level of the choanae and slightly separated from each other. Several small rounded teeth (4-6) are present in each vomer; tongue is wider than long, heart-shaped and jagged posteriorly, where also free along one-third of its length (Table 3).

Skin of the dorsum is shagreen, highly tuberculate towards the posterior region and smooth towards the anterior region, flanks bearing small, scattered tubercles; skin on throat, chest and belly areolate. Ventral surfaces of the thighs and concealed surfaces of the hindlimbs are areolate with a contrasting pattern consisting on dark brown mottling on light cream to dark brown background with irregular flecks and blotches. Discoidal fold is present and cloacal sheath short, skin of the upper cloacal region shagreen weakly tuberculate, and two distinct rounded tubercles below the cloacal sheath are surrounded by few smaller tubercles. Prominent ulnar tubercles surrounded by few small, rounded tubercles are present. Outer palmar tubercle is prominently heart-shaped, approximately twice of the thenar tubercle. Inner palmar tubercle prominent and elliptical, subarticular tubercles prominent, well defined and rounded in ventral and lateral view, supernumerary tubercles are present, rounded and darker. Fingers and toes are emarginated with narrow lateral fringes (less than twice of the width of the digit region proximal to fingers and toes discs); Finger I is shorter than Finger II; all finger discs are barely expanded and semi truncated with well-defined finger pads; circumferential grooves in all fingers are present (Fig. 3).



Figure 3. Coloration in life of *Pristimantis elquimi* sp. n. **A** dorsal view and **B** ventral view. From left to right: QCAZ 68544, SVL= 31.57, adult female; QCAZ 68545, SVL= 26.40, adult male; QCAZ 68546, SVL= 18.69, sub-adult male.

Hindlimbs are slender, tibia length is 57% of SVL, and foot length is 46% of SVL. Hindlimbs and flanks patterned, with transverse darker brown bars; ventral surface of the thighs is areolate, posterior surface of thighs is black with white spots, heel bears a prominent and conical, and well-defined tubercle surrounded by few small, rounded tubercles. Two prominent and subconical outer tarsal tubercles are present, but inner tarsal fold is absent. Inner metatarsal tubercle is prominent and elliptical, small ovoid, distinct outer metatarsal tubercles are present, plantar surface bears small rounded tubercles, subarticular tubercles are prominent, rounded in lateral and ventral views. Basal webbing in toes is absent, discs are slightly smaller than those on fingers, and well-defined disc pads are surrounded by circumferential grooves. Discs are expanded and rounded, more prominent on Toe IV and V. Toe V is longer than Toe III (disc on Toe III reaches the

middle of the penultimate subarticular tubercle on Toe IV, disc on Toe V extends to proximal edge of distal subarticular tubercle on Toe IV). Relative length of toes is the order I < II < III < V < IV (Fig. 4).

Color of the holotype in life (based on digital photographs) is as follows. Dorsal surfaces of body, limbs, fingers and toes are dark brown with lighter brown mottling. Top of the head medial to the orbits bears an interorbital dark brown bar with a prominent medial conical tubercle surrounded by light brown markings and a second medial tubercle, located anteriorly, vertically aligned with the interorbital tubercle and horizontally aligned with the anterior border of the eyes. Canthal stripe is light brown, and a dark brown marking with a small, rounded tubercle in the central region anterior to the interorbital bar is present. Scapula bears scatter W-shaped dermal crests (> < shape with an internal small V-shaped scapular fold) and two dark brown middorsal folds (see Fig. 5). Ventral region, throat, forelimbs, flanks, and groins are dark brown with brownish cream blotches. The border of the eyelid is outlined by a cream-colored line around the entire eye. Vertical labial bars are dark brown, supratympanic fold is brown, and hindlimbs are dark brown with light brown stripes that became blotches towards the concealed surface of shanks. Posterior surfaces of thighs have a dark brown color with small white dots.

Table 3. Measurements (in mm) and proportions of type series of *Pristimantis elquimi* sp. n. Ranges followed by means and one standard deviation in parameters. (**SVL** snout-vent length; **HL** head length; **HW** head width; **EW** upper eyelid width; **ED** eye diameter; **IOD** interorbital distance; **IND** internarial distance; **END** eye-nostril distance; **TL** tibia length; **FL** foot length; **TY** tympanic diameter).

	Males (n=2)	Females (n=1)	QCAZ 68544	QCAZ 68545	QCAZ 68546	Average	ED
SVL	26.4 – 18.69 (22.55 ± 5.5)	31.57	31.57	26.4	18.69	22.55	5.5
HL	8.43 – 6.61 (7.52 ± 1.3)	10.05	10.05	8.43	6.61	7.52	1.3
HW	9.58 – 7.14 (8.36 ± 1.7)	11.51	11.51	9.58	7.14	8.36	1.7
EW	2.73 – 2.08 (2.41 ± 0.5)	4.36	4.36	2.73	2.08	2.41	0.5

ED	3.76 – 2.99 (3.38 ± 0.5)	4.72	4.72	3.76	2.99	3.38	0.5
IOD	3.19 – 2.01 (2.60 ± 0.8)	3.59	3.59	3.19	2.01	2.60	0.8
IND	1.61 – 0.82 (1.22 ± 0.6)	2.04	2.04	1.61	0.82	1.22	0.6
END	3.66 – 2.53 (3.10 ± 0.8)	3.82	3.82	3.66	2.53	3.10	0.8
TL	15.69 – 11.26 (13.48 ± 3.1)	18.09	18.09	15.69	11.26	13.48	3.1
FL	12.73 – 8.95 (10.84 ± 2.7)	14.53	14.53	12.73	8.95	10.84	2.7
TY	1.72 – 0.83 (1.28 ± 0.6)	1.57	1.57	1.72	0.83	1.28	0.6
HL/SVL	0.32 – 0.35 (0.34 ± 0.0)	0.32	0.32	0.32	0.35	0.34	0.0
HW/SVL	0.36 – 0.38 (0.37 ± 0.0)	0.36	0.36	0.36	0.38	0.37	0.0
HW/HL	1.14 – 1.08 (1.11 ± 0.0)	1.15	1.15	1.14	1.08	1.11	0.0
EW/SVL	0.14 – 0.16 (0.15 ± 0.0)	0.15	0.15	0.14	0.16	0.15	0.0
END/ED	0.97 – 0.85 (0.91 ± 0.1)	0.81	0.81	0.97	0.85	0.91	0.1
EW/IOD	1.38 – 1.44 (1.41 ± 0.0)	1.08	1.08	1.38	1.44	1.41	0.0
TY/ED	0.46 – 0.28 (0.37 ± 0.1)	0.33	0.33	0.46	0.28	0.37	0.1

Variation. The description of the specimen's coloration in this section refers specifically to the preserved colors of the individuals examined (Fig. 5). Apparently, there is sexual dimorphism in body size. In the type series, adult males (26.4 – 18.69 mm) are smaller than the single known female (31.57 mm). See Table 3 for measurements and proportions (HL/SVL, HW/SVL, HW/HL, EW/SVL, END/ED, EW/IOD, TY/ED) of the type specimens. Males lack of vocal slits and nuptial pads. Ventral coloration pattern possess greater contrast and it is well defined in females and became a diffuse marbling in males (Figure 5). The adult male paratopotype (QCAZ 68545, SVL 26.40) presents a different ventral coloration pattern in that the blotches are more diffuse resembling more a marbled pattern (see also QCAZ 68546). Males possess more prominent dermal crests than the adult female holotype. The sub-adult male (QCAZ 68546 SVL 18.69) shows a cream-colored

vermiculated pattern that extends up to the interior of the venter. The two specimens are different from the holotype in being lighter (QCAZ 68545) and darker (QCAZ 68546) brown. Paratopotypes also have different blotching patterns than the female holotype in the flanks, inner surface of the thighs, and concealed surfaces of shanks. Labial bars are diffuse. All the specimens reveal a similar structure of dermal crests labial bars, ventral surface of the thighs, and ventral surfaces of the tarsus, forelimbs, and palms. Iris is reddish-brown all individuals (see Fig. 3).



Figure 4. Palmar and plantar surfaces of the new species. Photos of right hand (**A**) and left foot (**B**) of *P. elquimi* sp. n., QCAZ 68544 (holotype), adult female, Hand Length (HL) = 9.28 mm, Foot Length (FL) = 14.53 mm.



Figure 5. Coloration in preserved specimens of *Pristimantis elquimi* sp. n., **A** dorsal view, and **B** ventral view. From left to right: QCAZ 68544, SVL= 31.57, adult female; QCAZ 68545, SVL= 26.40, adult male; QCAZ 68546, SVL= 18.69, sub-adult male.

Osteological descriptions

The osteological descriptions are based on a micro-CT 3D reconstruction of the holotype (QCAZ 68544). We focus especially on cranial morphology, postcranial skeletal features, and osteological aspects of hand and foot.

Cranium and mandible. The skull is slightly wider than long, the widest part being the space between the most lateral bends of the quadratojugal, located approximately at the anterior tip of the squamosal, and reaching 97% of the length of the skull. The rostrum is short, with the distance from the front edge of the frontoparietals to the anterior face of the premaxilla comprising 23% of the length of the skull. At the midorbital level, the braincase is 39% of the maximum width of the skull (Fig. 6).

The braincase is partially well ossified. It features a pair of thickened cranial crests in the otoccipital bone, we suggest originated from the fusion of the prootic and the exoccipital. The frontoparietals are fully developed, longer than wide, being narrowest anteriorly and posteriorly with a partially ossified medial fontanelle along the medial section. The frontoparietals are completely fused. The posterior section of the brain box is enclosed by the fused frontoparietals and otoccipital. Two well defined ventrolateral small occipital condyles are present. The sphenoid is dorsally fused with the frontoparietals and ventrally with the parasphenoid; it is well ossified throughout. The sphenethmoid is not divided, being well ossified. The anterior margin of the parasphenoid begins slightly further back than the level at which the midpoint of the orbit is located, at this point it separates from the frontoparietals, but continues to contact the otoccipital posteroventrally. The cultriform process of the parasphenoid occupies about 17% of the width of the cerebral box at mid orbit and features parallel lateral margins. The wings of the parasphenoid are long and thickened posterodistally (each wing is longer than the cultriform process).

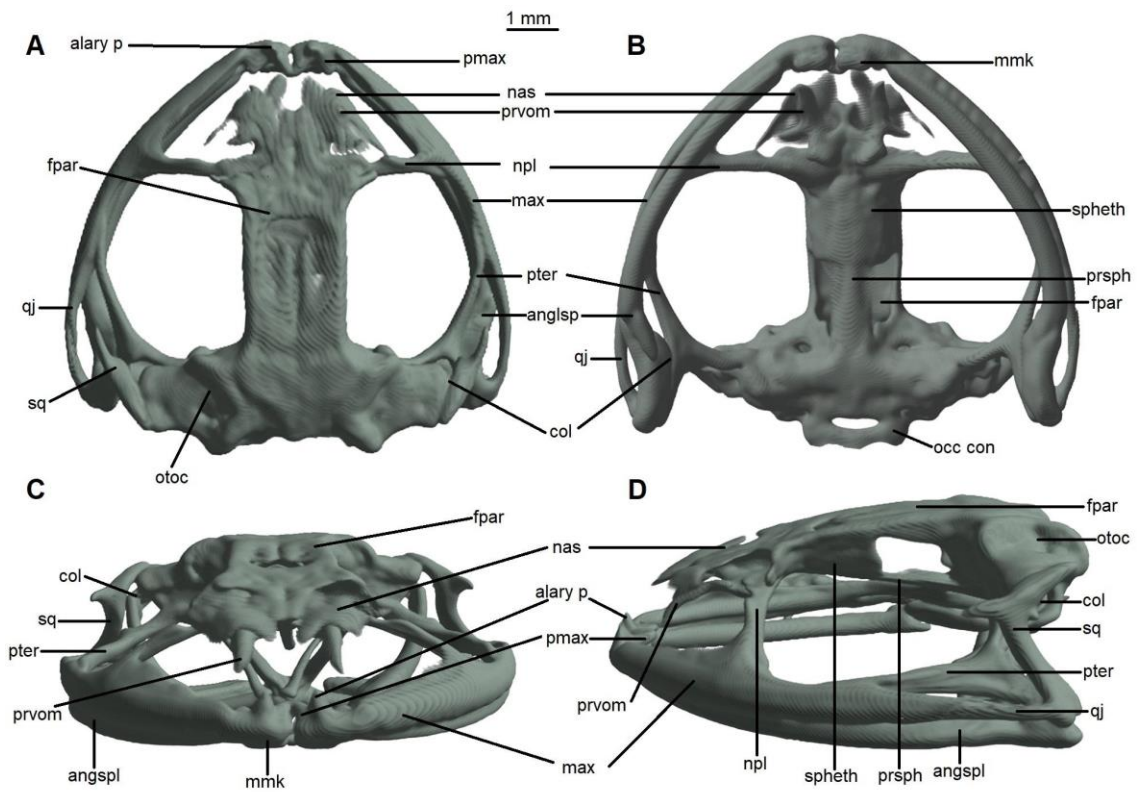


Figure 6. Head skeleton of *Pristimantis elquimi* sp. n. (holotype, QCAZ 68544). The skull

is shown in (A) dorsal, (B) ventral, (C) frontal, and (D) lateral views. alary p, alary process; angspl, angulosplenia; col, columella; fpar, frontoparietal; max, maxilla; mmk, mentomeckelian bone; nas, nasal; npl, neopalatine; occ con, occipital condyle; otoc, otoccipital (fused prootic and exoccipital); pmax, premaxilla; prsph, parasphenoid; prvom, prevomer; pter, pterygoid; qj, quadratojugal; spheth, sphenethmoid; sq, squamosal.

Well-defined neopalatines are dorsally connected to the sphenethmoid and centrally connected to the maxilla. Septomaxilla are not visible. Cranium possesses a large and well-ossified delineated columella. The columella (or stirrup) is large, well ossified and fused with the pterygoid. Nasals are semi-conic, wider than long, and centrally fused with each other. Besides, nasals presents an extensive bone narrowing at the back of the nostrils with a partial fusion to the front end of the frontoparietals, but with no connection to the maxilla. The prevomers appear fused with the nasals.

A partial medial separation of premaxillae is present, and their anterodorsal alary processes rise weakly away from the midline, but are distinctly separated from the nasal. The contact between maxilla and premaxilla is only by the juxtaposition of articulation. Posterior end of the jaw is semi-rounded with several points of contact with the quadratojugals. The triply forked pterygoid has a curved anterior branch with an anterolateral orientation pointing towards the maxilla; this bone formation generates the anteroventral corner of the ocular orbit. The anterior branch of the pterygoid is noticeably longer than the medial branch, whereas the posterior branch is slightly less robust than the medial branch. The edge of the medial branch overlap slightly in relation to the lateral edge of the otoccipital.

The quadratojugal is wide and elongated. Although it is not possible to see the joint this bone touches the T-shaped squamosal. The zygomatic branch is much smaller than the otic branch. The slightly serrated jaw is thickened. The mentomeckelians are longer than they are wide, not adjoined medially or laterally by ossified structures A curved and elongated angulosplenia exhibits a wide articulation with the denture. Coronoid process is long and slightly elevated. Information regarding the structure of tooth is limited but there have not contact with the mentomeckelian bones. Given the specimen was scanned with closed mandibula, teeth could not be counted. Posteromedial processes of hyoid apparatus are

ossified and narrow posteriorly, slightly expanded anteriorly, and moderately separated from one another at the anteriorly.

Postcranium. Eight vertebrae constitute the presacral. The first one is longer than the posterior ones. Vertebrae that do not belong to the Presacral I have slightly reduced diapophysis compared with Presacral I. Presacral I possesses a cross-sectional process and is anterolaterally pointed. There is a similarity in structure between Presacral II and III, Presacral II is longer and has a posterolateral orientation. Presacral I is relatively rounder and wider than Presacral II and III. Presacral II and III are more posterolaterally oriented than Presacral I. Also there is a change of orientation of Presacral IV and V, both have the same length, are narrower than Presacral II and III, are oriented at an increased angle in posterolateral direction, Presacral VI and VII have a similar orientation change, this time at an decreased angle into anterolateral direction, which produces a slightly alignment of these vertebrae on the horizontal axis. Presacral VIII does not have transversal processes. Presacrals I-III are thicker and broad than Presacrals V-VIII.

The diapophysis of the sacrum is slightly expanded. The diapophyses of the sacral vertebra (sacral diapophyses) are cylindrical, and both longer and wider than the presacral vertebrae. The urostyle is elongated and narrow. It is longer than the presacral region of the spine and has a well-pronounced dorsal crest. Sesamoid elements do not have ossified components. The presence of a bicondylar joint is presumed based on the bone structures of the new species' relatives within the Strabomantidae, as it is not completely visible in the computer microtomography (Reyes-Puig JP et al. 2019). The shoulder girdle consists of two elongated and thick clavicles, which are curved anteromedially. They are joined at the center, forming an inverted V-shaped structure. Coracoids are wider in the medial region and at distal ends. Central region is narrower than distal ends and the distal edge is curved.

The coracoid process is symmetrically separated posterolaterally in the pectoral girdle due to the epicoracoid cartilage. In this area, there are also the procoracoid cartilage, sternum and omosternum, all of which are not present in the reconstruction, suggesting the presence of cartilaginous elements in this structure. Coracoid process is slightly joined in the anteromedial region to the clavicles (Fig. 7). The glenoid end of the coracoid is slightly narrower than the sternal. Pars acromialis is in contact with pars glenoidalis. Scapula is

long and wide distally. Cleithrum is barely observable in computer microtomography. The hyoid apparatus is also not visible, which suggests that its structure is cartilaginous. Thyrohials or posteromedial processes are the only bones of the hyoid apparatus. Dorsolateral ridges on the iliac stems of the pelvic girdle are present, prominent, and found along 2/3 of their length.

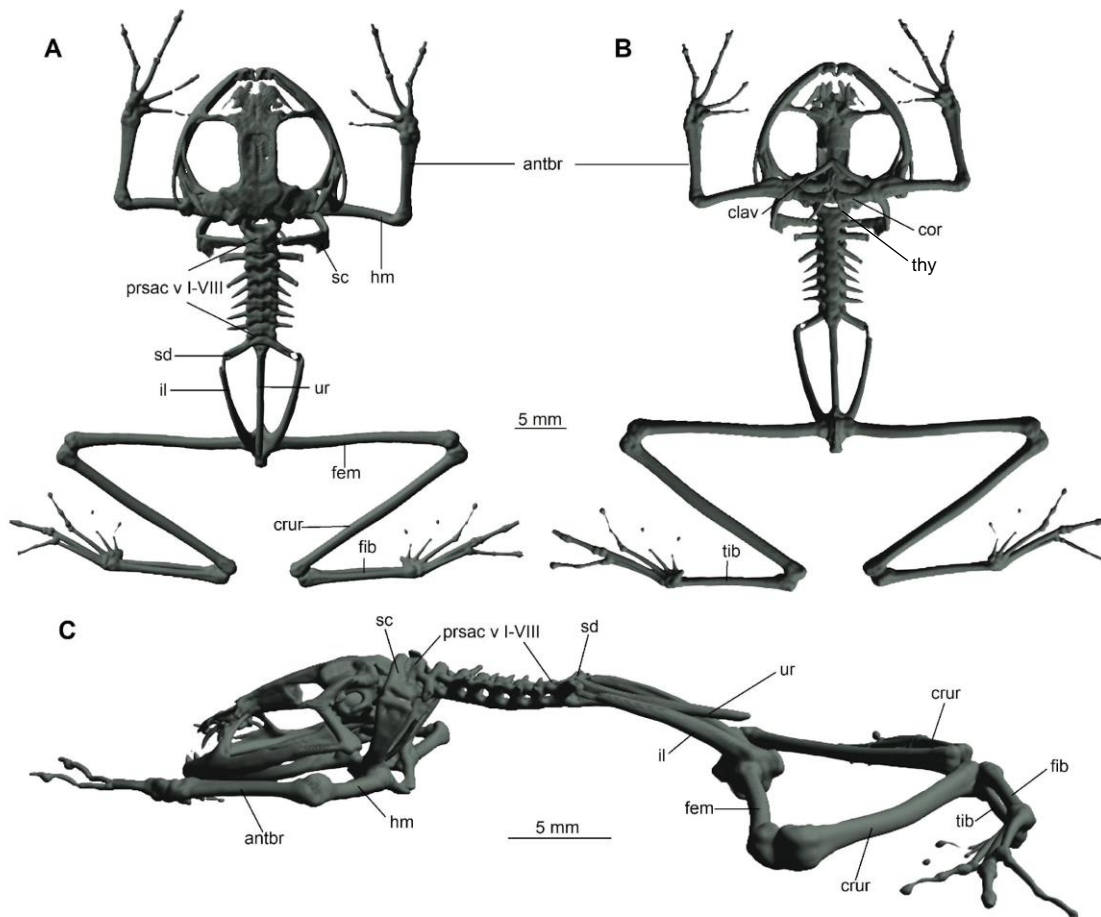


Figure 7. Osteology of *P. elquimi* sp. n. (holotype, QCAZ 68544). The full skeleton is shown in (A) dorsal, (B) ventral, and (C) lateral views. antbr, os antebrachii (radius + ulna); clav, clavicle; cor, coracoid bone; crur, os cruris (tibia + fibula); fem, femoral bone; fib, fibulare; hm, humeral bone; il, ilium; prsac v, presacral vertebrae I-VIII; sd, sacral diapophysis; sc, scapula; ur, urostyle; thy, thyrohials; tib, tibiale.

Manus and pes. The level of ossification of the phalanges is measured through the phalanx formula, describing how many phalanges appear ossified in each finger and toe: 2,2,3,3 and 2,2,3,3,3 going from finger I to IV and Toe I to V respectively (foot information

was compared with a juvenile specimen for more consistency in the osteological description, Toes from I to III partially visible in the holotype). In ascending order the relative lengths of the fingers are $I < II < IV < III$, and those of the feet are $I < II < III < V < IV$. A small distal protuberance is visible at the distal ends of the phalanges; however, the resolution of the reconstructions of the micro-CT bone structures is coarse. All the distal ends of the phalanges in hands and feet taper distally. Carpus and tarsus do not provide informative characters given the resolution of the micro CT scans (Fig. 8).

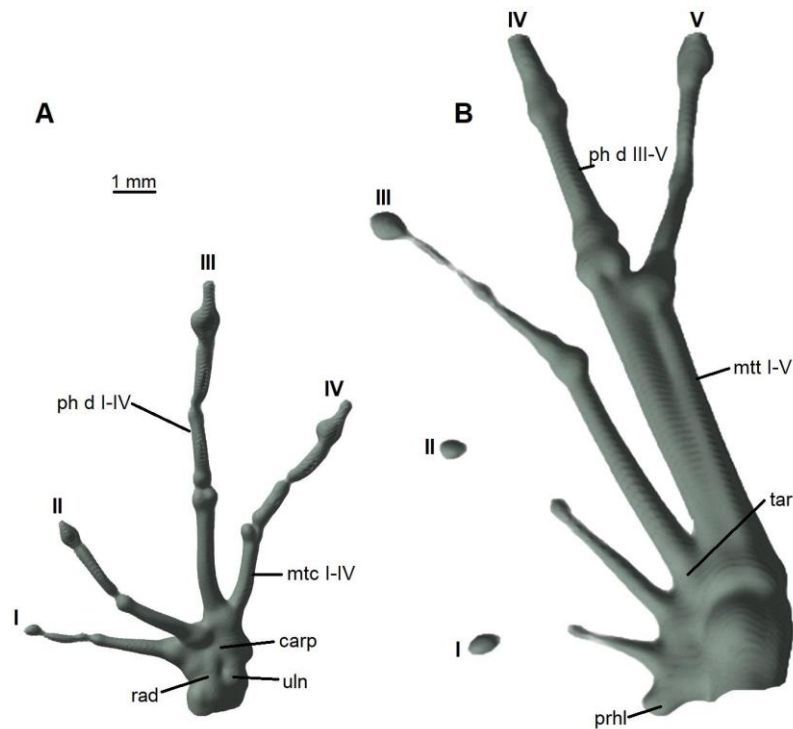


Figure 8. Osteology of the limbs of *P. elquimi* sp. n. (holotype, QCAZ 68544). (A) The left forelimb is shown in dorsal aspect; and (B) the right foot in dorsal aspect. Digits numbered I–IV; carp, carpal; mtc I–IV, metacarpalia F1–F4; mtt I–V, metatarsalia T1–T5; ph d I–IV, finger phalanges F1–F4; ph d III–V, toe phalanges F3–F5; prhl, prehallux, rad, radiale; tar, tarsale; uln, ulnare.

Distribution, natural story and conservation status

The known distribution of *P. elquimi* sp. n. is restricted to one locality (elevation range 1988–2200 m) on the Eastern slopes of the Cordillera del Cóndor, Ecuador, Morona Santiago Province, in the El Quimi Ecological Reserve buffer zone, on the tepuy plateau on the eastern side of the Quimi River Valley, next to the Río Cristalino de Aguas Negras with fords (white foam) on the edges. The predominant ecosystem is Evergreen Montane Forest of the Eastern Andean Cordillera as defined by Ministerio de Ambiente del Ecuador (2013) or Eastern Montane Forest as defined by Ron et al. (2018).

The Condor Cordillera represents a unique ecosystem made up of Sandstone Mountains. It has the exceptional attribute of being the most diverse area of all the Andes. 27% of the herpetofauna of the area is endemic. Its geological structure presents tepuis, high and flat plateaus of the mountains, that allow the development of habitats similar to the tepuis of the Guyanas' shield from the Venezuelan Gran Sabana. The forest full of stunted trees, mosses, lichens, and epiphytes on limestone rocks make up a landscape unique in the country. The edaphic-geological characteristics of the soil, such as the presence of limestone generate a high level of floral endemism which correlates with the wide variety of fauna species found in the place, the reason why it is imperative the conservation of the so unique biodiversity so unique that it has the area. The tributaries of water belonging to this cordillera feed extensive territories occupied by indigenous and colonizing communities, as well as the forest resources are indispensable for their subsistence. In 1997, this area was reported as relatively pristine. However, today great mining projects such as the Proyecto Mirador, located 8 km from the type locality of the new species (Fig. 9) flatly threaten the biodiversity of the area (Conservation International 1997).

The holotype and the paratopotypes were collected on vegetation at night. The locality is a firm ground forest. All the specimens were collected in an area with shrubby understory (height 1.50 m) and highly space, 10-15 m high trees with slim stems widely spaced from each other. This area is covered by abundant moss and bromeliads on bamba soil (padded soil with abundant roots and many cavities in between; 70% root to 30% earth).

Pristimantis elquimi sp. n. was found in moss 40 cm above the ground.

According to the available information, the Quimi Valley represents a geographical barrier, confining this frog's distribution. Due to the lack of population data, we assign *P. elquimi* sp. n. to the Data Deficient Red List Category (IUCN 2017).

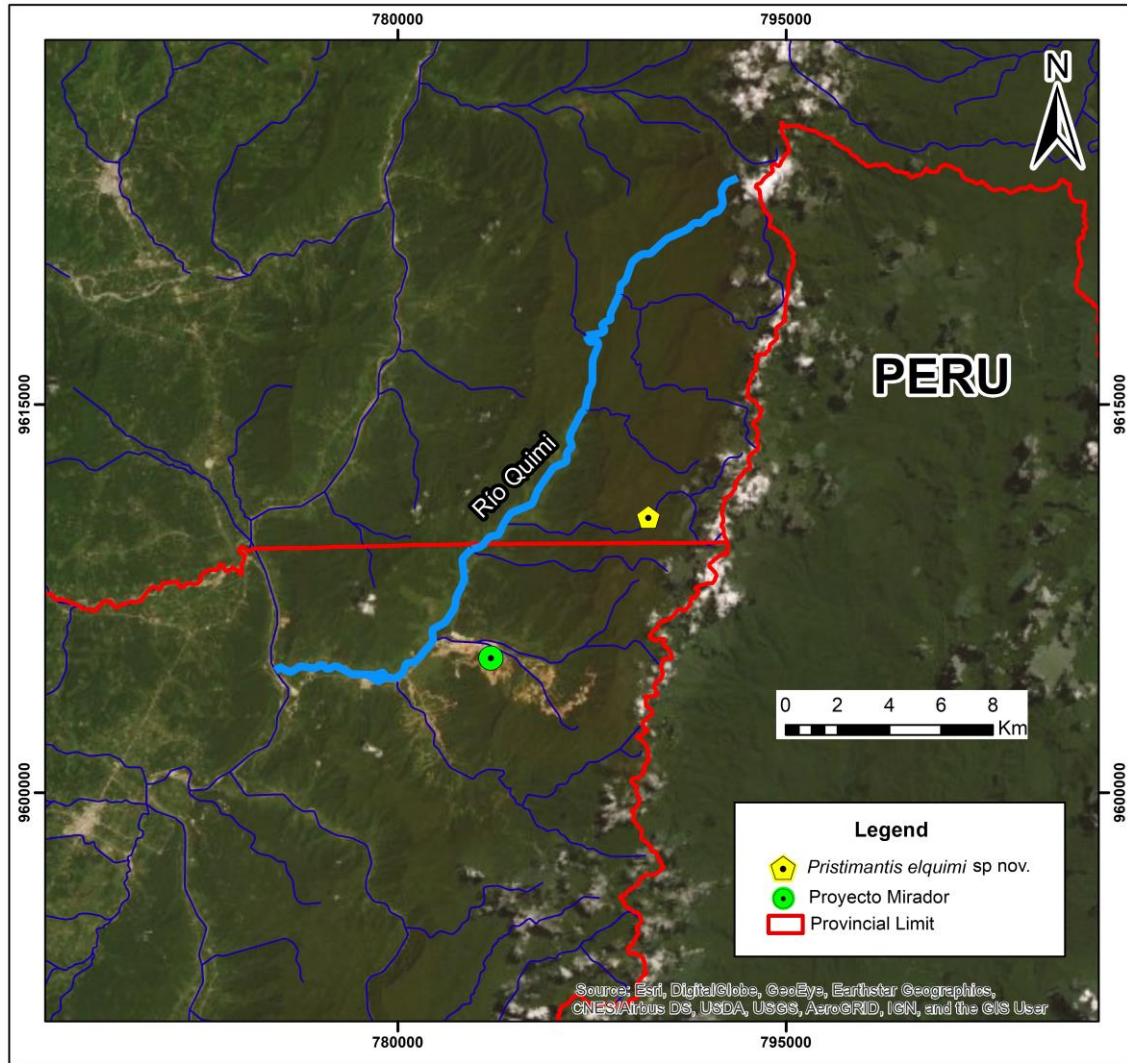


Figure 9. Map of deforestation processes adjacent to the type locality of *P. elquimi* sp. nov.

Etymology

The specific name *elquimi* is a noun that represents the type locality, the Quimi Valley. It is part of the El Quimi Ecological Reserve, managed by the Ministerio del Ambiente of Ecuador. It was created to protect the eastern montane forests of the Quimi basin.

Pristimantis elquimi sp. n. bears that name to attract attention to the Quimi Valley buffer zone, which is in dire need of conservation action. The ecosystems of the Cordillera del

Condor are increasingly threatened by anthropogenic activities such as deforestation, agriculture and extractive activities.

Discussion

The present phylogeny shows the monophyly of the subgenus *Huicundomantis*, confirms the status of the species groups' as proposed by Páez and Ron (2019). This article elucidated information regarding morphological and phylogenetic relationships of *P. muscosus* species and what we determinate as its sister clade and most related species. We suggest that specimens identified as *P. muscosus* from Yacuri National Park might not be *P. muscosus* sensu stricto due to their highly variable morphological traits when compared to the *P. muscosus* holotype from the eastern slope of Abra Pardo San Miguel in Peru. However, a complete phylogenetic study is needed to clarify the taxonomic status of those specimens.

The morphological relationship established between the species belonging to the *P. cryptomelas* species group could be useful for future research. Páez and Ron (2019) systematic study of the *P. cryptomelas* group based on DNA sequences supports *P. elquimi* sp. n. as a new species. Given the isolation of the type locality of *P. elquimi* sp. n and the limited number of faunal inventories, the discovery of more new species is expected. *Pristimantis* is characterized by high levels of endemism influenced by altitudinal variations in physiography. Both morphological and osteological descriptions yield useful information for the systematics of the species. The present osteological description lay the basis for future comparative analyses in trait evolution. Also, the osteological description of *Pristimantis* might help to provide new insights into the primitiveness state of some terrarana representative characters. More osteological descriptions could improve our understanding of evolutionary trends in the osteology of the genus *Pristimantis*.

The discovery of new species of amphibians in areas such as the El Quimi Valley will be useful for the improvement of public policies regarding biodiversity conservation in the Cordillera del Condor (Yanez-Muñoz et al., 2010; Neill, 2015; Páez & Ron, 2019). The discovery of a cluster of endemic species highlights the conservation value of the valley and the need for more faunal surveys and collection of population level data for the local

herpetofauna. Contamination of the Quimi River due to mining poses one of the greatest threats to biodiversity at this locality.

Conclusion

We present *Pristimantis elquimi* sp. n. based on morphological, osteological, and genetic information. This work supports the validity of the subgenus *Huicundomantis* as a monophyletic clade formed by two distinctive species groups: *P. cryptomelas* and *P. phoxocephalus*. The lack of tissue samples from the holotype of *P. muscosus* somewhat hampers our interpretations. The tepuy plateau of the Quimi Valley is home to a large number of undescribed species due to its isolated physiography. For this reason it is important to conserve the area. Further studies are recommended to provide an accurate picture of the status of *P. muscosus* in Ecuador. More research on osteological traits in modern anurans are needed to assess the usefulness of traits evolution for basal terrarana anurans.

Acknowledgments

We thank the members of the Museo de Zoología of the Pontificia Universidad Católica del Ecuador (PUCE) for their work in the conservation of the Ecuadorian Biodiversity, Fernando Ayala, Diego Almeida, Maria Jose Navarrete, Jhael Ortega, Yerka Sagredo, and Julio Carrión. The members of the Molecular Biology Laboratory of the Museo de Zoología, Claudia Terán and Ana Belen Carrillo for their assistance when needed. We are very grateful to Mario Yáñez Muñoz from the Instituto Nacional de Biodiversidad (INABIO) for institutional support in the realization of the phylogeny and morphological descriptions. We are grateful to the School of Earth and Energy Sciences at Yachay Tech for letting us use the nanotomographer and specifically Elizabeth de las Mercedes Mariño Morejón for scanning the species. Also, thanks to Ana Almendariz from the Escuela Politécnica Nacional (EPN) and Markus Tellkamp read the manuscript and provided valuable comments.

References

- AmphibiaWeb. 2019. <<https://amphibiaweb.org>> University of California, Berkeley, CA, USA. Accessed 10 Jun 2019.
- Brito, J., & Almendáriz, A. (2018). Una especie nueva de rana *Pristimantis* (Amphibia: Strabomantidae) de ojos rojos de la Cordillera de Cóndor, Ecuador. Cuad. herpetol. 32(1): 31-40., DOI: 10.31017/cdh.2018.(2017-08)
- Brito, J., Batallas D., & Yáñez-Muñoz M. H. (2017). Ranas terrestres *Pristimantis* (Anura: Craugastoridae) de los bosques montanos del río Upano, Ecuador: Lista anotada, patrones de diversidad y descripción de cuatro especies nuevas, Neotropical Biodiversity 3(1): 125-156, DOI: 10.1080/23766808.2017.1299529
- Bruker. (2016, July). NRecon User Manual. User manual for SkyScan reconstruction program NRecon.
- Conservation International Department of Conservation Biology (1997) The Cordillera del Cóndor Region of Ecuador and Peru: A Biological Assessment
https://bibdigital.epn.edu.ec/bitstream/15000/4752/1/RAP07_Cordillera_Condor_Ecuador-Peru_Jan-1997.pdf [Accessed on: 2020-05-16]
- CTan (Version N° 1.18.8). (2018). Windows. Billerica, Massachusetts, USA: Bruker.
- CTvox (Version N° 3.3). (2016). Windows. Billerica, Massachusetts, USA: Bruker.
- Chernomor, O., von Haeseler, A., & Minh B.Q. (2016). Terrace aware data structure for phylogenomic inference from supermatrices. Systematic Biology 65: 997-1008, <https://doi.org/10.1093/sysbio/syw037>
- Duellman, W. E., & Lehr, E. (2009). Terrestrial-breeding frogs (Strabomantidae) in Peru. Münster: Germany: Nature und Tier Verlag.

- Duellman, W. E., & Pramuk, J. B. (1999). Frogs of the genus *Eleutherodactylus* (Anura: Leptodactylidae) in the Andes of northern Peru. *Scientific Papers. Natural History Museum, University of Kansas* 13: 1-78, <https://doi.org/10.5962/bhl.title.16169>.
- Frost, D. R. 2016. (2016). *Amphibian Species of the World: an Online Reference*. Version 6.0 Accessed on 13 August 2016. Electronic Database accessible at <http://research.amnh.org/herpetology/amphibia/index.html>. American Museum of Natural History, New York, USA.
- Frost, D. R. (2018, August 13). *Amphibian Species of the World: an Online Reference*. Version 6.0. Retrieved from American Museum of Natural History, New York, USA.: Electronic Database accessible at <http://research.amnh.org/herpetology/amphibia/index.html>.
- Geneious (Version N° 5.4.6). (2019). Mac. GeneMatters Corp.
- Guayasamin, J. M., Krynak, T., Krynak, K., Culebras, J., & Hutter, C. R. (2015). Phenotypic plasticity raises questions for taxonomically important traits: a remarkable new Andean rainfrog (*Pristimantis*) with the ability to change skin texture. *Zoological Journal of the Linnean Society* 173: 193-198. doi: <https://doi.org/10.1111/zoj.12222>
- Guindon, S., Dufayard, J.-F., Lefort, V., Anisimova, M., Hordijk, W., & Gascuel, O. (2010, May). New Algorithms and Methods to Estimate Maximum-Likelihood Phylogenies: Assessing the Performance of PhyML 3.0. *Systematic Biology* 59(3): 307-321. doi:<https://doi.org/10.1093/sysbio/syq010>
- Hedges, S. B., Duellman, W. E., & Heinicke, M. P. (2008). New World direct-developing frogs (Anura: Terrarana): molecular phylogeny, classification, biogeography and conservation. *Zootaxa* 1737: 1-182.
- Heinicke, M. P., Duellman, W. E., & Hedges, S. B. (2007). Major Caribbean and Central American frog faunas originated by ancient oceanic dispersal. *Proceedings of the*

National Academy of Sciences of the United States of America, (Supplemental Online Information) 104. doi:10.1073/pnas.0611051104

Hoang, D. T., Chernomor, O., Haeseler, A. v., Minh, B. Q., & Vinh, L. S. (2018, February). UFBoot2: Improving the Ultrafast Bootstrap Approximation. *Molecular Biology and Evolution* 35(2): 518-522. doi:<https://doi.org/10.1093/molbev/msx281>

IUCN Standards and Petitions Subcommittee (2017) Guidelines for Using the IUCN Red List Categories and Criteria. Version 13. Prepared by the Standards and Petitions Subcommittee. <http://www.iucnredlist.org/documents/RedListGuidelines.pdf>. [Accessed on: 2019-12-06]

Katoh, et al. (2002). MAFFT (Version N° 6.814b). Windows.

Lynch, J. D. (1979). Leptodactylid frogs of the genus *Eleutherodactylus* from the Andes of southern Ecuador. *Miscellaneous Publication. Museum of Natural History, University of Kansas* 66: 1-62.

Lynch, J. D., & Duellman, W. E. (1980). The *Eleutherodactylus* of the Amazonian slopes of the Ecuadorian Andes (Anura: Leptodactylidae). *Miscellaneous Publication Natural History Museum* 69: 1-86.

Lynch, J. D., & Duellman, W. E. (1997). Frogs of the genus *Eleutherodactylus* in western Ecuador. Systematics, ecology, and biogeography. *Special Publication. Natural History Museum, University of Kansas* 23: 1-236. doi:<https://doi.org/10.5962/bhl.title.7951>

Mesquite (Version N° 3.6). (2018). Windows. Madison and Madison.

Minh, B. Q., Nguyen, M. T., & Haeseler, A. v. (2013, May). Ultrafast Approximation of Phylogenetic Bootstrap. *Molecular Biology and Evolution*, 30(5), 1188-1195. doi:<https://doi.org/10.1093/molbev/mst024>

Ministerio de Ambiente del Ecuador (2013) Sistema de Clasificación de los Ecosistemas del Ecuador Continental. Subsecretaría de Patrimonio Natural, Quito, Ecuador.

- Ministerio del Ambiente. (2019, June 11th). Sistema Nacional de Areas Protegidas. Retrieved from Reserva Biológica: <http://areasprotegidas.ambiente.gob.ec/es/areas-protegidas/reserva-biol%C3%B3gica-el-c%C3%B3ndor>
- Navarrete, M. J., Venegas, P. J., & Ron, S. R. (2016). Two new species of frogs of the genus *Pristimantis* from Llanganates National Park in Ecuador with comments on the regional diversity of Ecuadorian *Pristimantis* (Anura, Craugastoridae). *ZooKeys* 593: 139-162. doi: 10.3897/zookeys.593.8063
- Neill, D. (2005). BOTANICAL TREASURES BETWEEN THE ANDES AND THE AMAZON. *PlantTalk* 41: 17-21.
- Nguyen, L.-T., Schmidt, H. A., Haeseler, A. v., & Minh, B. Q. (2015). IQ-TREE: A Fast and Effective Stochastic Algorithm for Estimating Maximum-Likelihood Phylogenies. *Molecular Biology and Evolution* 32(1): 268-274. doi:<https://doi.org/10.1093/molbev/msu300>
- NRecon (Version N° 1.7.4.2). (2016). Windows. Billerica, Massachusetts, USA: Bruker.
- Padial, J. M., Grant, M. T., & Frost, D. R. (2014). Molecular systematics of terraranas (Anura: Brachycephaloidea) with an assessment of the effects of alignment and optimality criteria. *Zootaxa* 3825: 1-132.
- Páez, N. B., & Ron, S. R. (2019). Systematics of *Huicundomantis*, a new subgenus of *Pristimantis* (Anura, Strabomantidae) with extraordinary cryptic diversity and eleven new species. *ZooKeys*.
- Pinto-Sanchez, N. R., Madrinan, S., Sanjur, O. I., Bermingham, E., & Crawford, A. J. (2012). The Great American Biotic Interchange in frogs: multiple and early colonization of Central. *Molecular Phylogenetics and Evolution* 62: 974-972. doi:10.1016/j.ympev.2011.11.022
- Pyron, R. A. (2014). Biogeographic analysis reveals ancient continental vicariance and recent oceanic. *Systematic Biology*, syu042. doi:10.1093/sysbio/syu042

- Pyron, R. A., & Wiens, J. J. (2011). A large-scale phylogeny of Amphibia with over 2,800 species, and a revised classification of extant frogs, salamanders, and caecilians. *Molecular Phylogenetics and Evolution* 61: 543-583.
doi:10.1016/j.ympev.2011.06.012
- Reyes-Piug, J. P., Reyes-Piug, C., Ron, S., Ortega, J. A., Guayasamin, J. M., Goodrum, M., . . . Yáñez-Muñoz, M. H. (2019). A new species of terrestrial frog of the genus *Noblella* Barbour, 1930 (Amphibia: Strabomantidae) from the Llanganates-Sangay Ecological Corridor, Tungurahua, Ecuador. *PeerJ*: 1-26. doi:10.7717/peerj.7405
- Ron, S. R., Merino-Viteri, A., & Ortiz, D. A. (2018, October 3). Anfibios del Ecuador. Version 2018.0. Retrieved from Museo de Zoología, Pontificia Universidad Católica del Ecuador. : <https://bioweb.bio/faunaweb/amphibiaweb>
- University of California, Berkeley, CA, USA. (2019, June 10). AmphibiaWeb. Retrieved from <https://amphibiaweb.org>
- Yáñez-Muñoz, M. H., Meza-Ramos, P., Cisneros-Heredia, D. F., & P, J. P. (2010, March 02). Descripción de tres nuevas especies de ranas del género *Pristimantis* (Anura: Terrarana). *Avances en Ciencias e Ingenierías*, 2(3), B16-B17. Retrieved from <http://revistas.usfq.edu.ec/index.php/avances/article/download/40/42>
- Yáñez-Muñoz, M. H., Sanchez-Nivicela, J. C., & Reyes-Piug, C. (2016). Tres nuevas especies de ranas terrestres *Pristimantis* (Anura: Craugastoridae) de la Provincia de El Oro, Ecuador. *Avances en Ciencias e Ingenierías* (Print: 1390-5384 Online: 2528-7788) 8(1): 5-25.
- Yáñez-Muñoz, M. H., Toral-Contreras, E., Meza-Ramos, P. A., Reyes-Puig, J. P., Bejarano-Muñoz, E. P., Mueses-Cisneros, J. J., & Paucar, D. (2012). New country records for five species of *Pristimantis* Jiménez. *Check List Journal of species lists and distribution* 8(2): 286-290.

Supplementary Information 1

Primers used for DNA PCRs

Authors: Odalys Torres, Santiago R. Ron

Explanation note: List of primers used for DNA amplicons generation.

Copyright notice: This dataset is made available under the Open Database License (<http://opendatacommons.org>). The Open Database License (ODbL) is a license agreement intended to allow users to freely share, modify, and use this Dataset while maintaining this same freedom for others, provided that the original source and author(s) are credited.

Link

Supplementary Information 2

Genetic distances

Authors: Odalys Torres, Santiago R. Ron

Explanation note: Table of genetic distances based in 16S gene. *Pristimantis* sp. nov. 3 description support.

	QCAZ 68546 <i>P. elquimi</i>	QCAZ 54857 <i>Pristimantis</i> sp. nov. 3	QCAZ 16448 <i>P. gloria</i>	QCAZ 45178 <i>P.</i> <i>jimenezi</i>	QCAZ 69189 <i>Pristimanti</i> sp. nov. 2	QCAZ 76129 <i>P.</i> <i>barrigai</i>	QCAZ 74686 <i>Pristimanti</i> sp. nov. 1	QCAZ 61252 <i>P. muscosus</i>	QCAZ 61249 <i>P. muscosus</i>
QCAZ 68546 <i>P. elquimi</i>	0.0000	0.0352	0.0958	0.1061	0.1429	0.0720	0.0630	0.0411	0.0424
QCAZ 54857 <i>Pristimanti</i> s sp. nov. 3	0.0352	0.0000	0.0955	0.1049	0.1399	0.0609	0.0664	0.0346	0.0360
QCAZ 16448 <i>P. gloria</i>	0.0958	0.0955	0.0000	0.0631	0.1450	0.1146	0.0819	0.0851	0.0851
QCAZ 45178 <i>P. jimenezi</i>	0.1061	0.1049	0.0631	0.0000	0.1672	0.1193	0.0965	0.0977	0.0988
QCAZ 69189 <i>Pristimanti</i> s sp. nov. 2	0.1429	0.1399	0.1450	0.1672	0.0000	0.1490	0.1357	0.1295	0.1302
QCAZ 76129 <i>P. barrigai</i>	0.0720	0.0609	0.1146	0.1193	0.1490	0.0000	0.0832	0.0449	0.0462
QCAZ 74686 <i>Pristimanti</i> s sp. nov. 1	0.0630	0.0664	0.0819	0.0965	0.1357	0.0832	0.0000	0.0574	0.0586
QCAZ 61252 <i>P.</i> <i>muscosus</i>	0.0411	0.0346	0.0851	0.0977	0.1295	0.0449	0.0574	0.0000	0.0000
QCAZ 61249 <i>P.</i> <i>muscosus</i>	0.0424	0.0360	0.0851	0.0988	0.1302	0.0462	0.0586	0.0000	0.0000